Journal of Atmospheric and Solar-Terrestrial Physics 71 (2009) 1814–1823

Contents lists available at ScienceDirect

Journal of Atmospheric and Solar-Terrestrial Physics

journal homepage: www.elsevier.com/locate/jastp

Influence of solar wind parameters on ground magnetic field near equator during intense storms

Geeta Vichare *[,1], S. Alex, G.S. Lakhina

Indian Institute of Geomagnetism, Navi Mumbai 410 218, India

ARTICLE INFO

Article history:
Received 25 November 2008
Received in revised form
2 April 2009
Accepted 30 June 2009
Available online 14 July 2009

Keywords:
Low-latitude magnetic field variations
Solar wind-magnetosphere interactions
Intense geomagnetic storms
Solar wind parameters

ABSTRACT

Using a simple time-lagged correlation technique, present study aims to identify the solar wind (SW) parameter, which is better associated with the ground magnetic field variations of shorter time duration near equator, during intense geomagnetic storms. It is found that out of all SW parameters, successively occurring enhancements in the SW dynamic pressure have substantial influence on the horizontal component of magnetic field at ground. Present analysis reveals a time lag of ~30–45 min between the SW pressure changes seen at L1 location and ground magnetic field variations, and hence providing a good approximation of an averaged propagation time during entire storm interval; the time lag varies with solar wind velocity. Separate study during day and nighttime suggests that the SW dynamic pressure enhancements recorded by the dayside outer magnetospheric satellite have impact on the ground horizontal magnetic field measurements near equator, irrespective of day or nighttime.

1. Introduction

During geomagnetic storm periods, the horizontal component of the magnetic field at low latitudes shows typical signature, understood to be associated with the development and decay of the ring current, which is fundamentally controlled by the southward turning of the interplanetary magnetic field (Tsurutani and Gonzalez, 1997; Gonzalez et al., 1999). Dst (or Sym-H) index is considered as a measure of the intensity of the ring current circulating symmetrically around the globe. However, the ring current is highly non-symmetric during the main and early recovery phase of the geomagnetic storms (Fukushima and Kamide, 1973; Liemohn et al., 2001; Ebihara et al., 2002) and this asymmetric component of ring current is given by ASY-H index. Besides this, it is often observed that the ground magnetograms show sudden impulses caused by the passage of interplanetary shocks and also reveal quasi-periodic structures, whose strength and appearance vary from station to station. Thus, during geomagnetically active periods the geomagnetic response to the solar wind (SW) consists of global, as well as local features. The global features are in general captured by geomagnetic indices computed from magnetic field variations at the ground-based stations distributed around the globe. However, the local features have to be dealt with special attention.

In the literature, the variations of the geomagnetic field have been discussed in terms of SW parameters by a number of researchers (Ogilvie and Burlaga, 1974; Russell et al., 1992, 1994; Korotova and Sibeck, 1995; Francia et al., 1999; Vichare and Alex, 2006). Most of these studies affirm the close association of geomagnetic field variations at various spatial locations, such as geosynchronous altitude, and high and low latitudes, with SW parameters. It is recognized that successively occurring enhancements in the SW dynamic pressure have a major impact on the magnetic field at ground. A lot of work has been carried out to investigate its effect on the Earth's magnetospheric–ionospheric current systems and corresponding magnetic field variations (Francia et al., 1999; Zesta et al., 2000; McPherron and O'Brien, 2001; Kepko and Spence, 2003; Wang et al., 2003; Lee and Lyons, 2004; Shi et al., 2005, 2006). All these studies suggest that the SW effects on the geomagnetic field may include magnetopause currents, as well as tail current and reconnection-related field-aligned currents. The response of the geomagnetic field to SW pressure variations is found to have a very clear one-to-one correspondence during northward IMF (Francia et al., 1999; Russell et al., 1994), however the complexities involved during southward IMF necessitate more cautious study during geomagnetically disturbed days. Lee and Lyons (2004) have studied the response separately during southward and northward IMF. They found that during southward IMF, the response to SW pressure pulses is mostly compression on dayside and change is dipolarization-like (similar to substorm response) on nightside; whereas during northward IMF, SW pressure enhancements generally lead to magnetic compression, with a few cases of

* Corresponding author.
E-mail address: geeta@iigs.iigm.res.in (G. Vichare).
[1] Earlier Geeta Jadhav.

1364-6826/$ - see front matter © 2009 Elsevier Ltd. All rights reserved.
doi:10.1016/j.jastp.2009.06.015

depression on the nightside, neither of which was a substorm-type of response. Villante et al. (1998) have studied geomagnetic field response at ground during severe geomagnetic activity associated with magnetic cloud and observed the same features at low and very high latitude stations that are associated with the SW changes. Also, many studies have been initiated to understand the day–night response to the SW parameters (Francia et al., 1999; Russell et al., 1994; Lee and Lyons, 2004; Shi et al., 2008a,b). It has been reported that at the geosynchronous orbit, sudden impulses had sparse effect near midnight (Nagano and Araki, 1986; Kokubun, 1993), whereas Francia et al. (1999) found the geomagnetic field response is greater around local noon and midnight, contrary to the findings of Russell et al. (1994), who found single peak near local noon. Shi et al. (2008a, b) attempted to model the geomagnetic field response to SW pressure enhancements due to various magnetospheric current systems, during different phases of the storm and discussed the differences in the MLT distribution of the ground response.

While analyzing intense magnetic storms near solar maximum of solar cycle 23, i.e., for the period between 1998 and 2001 (Vichare et al., 2005), we noticed some variations on a time scale of a few minutes, in the low-latitude ground magnetic field, which is a commonly observed feature during storm interval (Kleimenova et al., 2002; Takahashi and Ukhorskiy, 2007); and at the first glance appeared to have some connection with the solar wind pressure. Since the Earth's magnetosphere is a complex dynamical system driven by the solar wind, the studies using correlated database of the solar wind–geomagnetic system could be helpful in understanding its complexity. Therefore, in the present paper, we use one-minute data at Alibag (Geomag. Latitude ~10°N, Geographic Longitude ~72.9°E) ground observatory and on-board ACE satellite measurements of the solar wind and interplanetary magnetic field parameters. Use of Alibag magnetic field variations for this type of study has been done for the first time. Since the geomagnetic field response to the SW pressure impulses has strong local time (Shi et al., 2008a), as well as latitudinal dependence (Rastogi, 1999), it is very important to examine the response near equator. Comparison of the variations observed in the residual ground magnetic field with that of the SW parameters and their spectral characteristics are discussed in Sections 2 and 3 respectively. Though it is known that the successively occurring enhancements in the SW dynamic pressure have considerable effect on the ground magnetic field variations, in the present investigation we intend to examine this through a simple time-lagged correlation technique, as described in Section 4. Use of this technique has been done extensively to monitor the solar wind plasma conditions at L1 point and near Earth location (Richardson et al., 1998; Paularena et al., 1998; Farrugia et al., 2005). Here, we apply the same technique to SW conditions at ACE location, i.e., L1 point and ground magnetic field variations near equator. This procedure could provide a good estimate of average time taken for the propagation from the L1 point to the ground during storm interval. In order to probe the contribution from differences in local time component, we further study the day and night sectors separately in Section 5. Finally, Section 6 summarizes and discusses the results.

2. Comparison between residual H and solar wind parameters

For the present study, we consider six intense geomagnetic storm events. One-minute data of horizontal magnetic field at Alibag observatory for two complete days (48 hours) are considered, which in general, comprises SSC, initial, main and partial recovery phase (first two, only when present). In the present paper we desire to study the geomagnetic field variations of timescale of a few minutes (<35 min). The ring current dependent magnetic field variations at low latitudes are basically long term (>1 h). Since in the present investigation, the data of two complete days are considered, diurnal or ionospheric variations are also present and are much stronger near the dip equator. These can mask the magnetic field variations of smaller scales, and therefore it is required to remove their effects. Most of the earlier studies (e.g. Francia et al., 1999; Villante et al., 2007) employed low-latitude stations at ~36°N geomagnetic latitude, with smaller time intervals, where effects of quiet time ionospheric currents were negligible. However, for the present study, we consider the quiet time and Dst variation as a natural background and we eliminate these background variations to delineate the information about small-scale variations of the magnetic field. There are two ways of removing the long period ionospheric and magnetospheric variations, viz. eliminating Dst and quiet day diurnal variation from the storm time magnetic field variations and another one is by directly using high-pass filter. Though latter is a more convenient way, it would be interesting to display the output obtained from the first option. Fig. 1 depicts the time series after systematic removal of the long period variations for the event on 24–25 September 1998. Top most plot (Fig. 1(a)) shows temporal variation of the horizontal component of magnetic field at Alibag during the above mentioned disturbed event. Fig. 1(b) shows the variation of H-component at Alibag during first quiet day of September 1998, which is 14 September 1998. Third plot (Fig. 1(c)) shows the variation after removal of quiet day pattern from the disturbed day variation, i.e., plot of Fig. 1(c) is obtained by subtracting plot 1(b) from 1(a). Fig. 1(d) depicts the Dst-index during the event. Dst reached a minimum of -207 at ~10 UT on September 25. The residual field (shown in Fig. 1(e)) is obtained after subtracting Dst-index from Fig. 1(c). The ground data used here has resolution of one minute, while Dst is hourly index. Therefore, in order to subtract the long period ring current contribution from the ground magnetic field data, we used interpolated values of the Dst-index. Since Sym-H index can contain the smaller period variations that need to be retained, as it is the main focus of the present paper, we found it appropriate to subtract the interpolated Dst values. SW parameters such as SW density, dynamic pressure, southward component of IMF ($B_{\mathrm{IMF,Z}}$), SW velocity, and temperature are depicted in Fig. 1(f)–(j) respectively. This particular event is very well investigated for the effects of the geomagnetic storm along with a classical SSC, on the Earth's magnetosphere–ionosphere system using multi-satellite and ground observations (Russell et al., 1999, 2000; Moore et al., 1999; Chi et al., 2000; Shi et al., 2008a). The magnetic storm began with the arrival of a sudden impulse at 23:45 UT on September 24, which abruptly increased the solar wind dynamic pressure on the nose of the magnetosphere from 2 to 15 nPa. After a sudden impulse, Bz was highly fluctuating between northward and southward orientation for an hour and then turned southward, attaining maximum value of 23 nT at ~0130 UT on 25 September 1998.

The residual magnetic field (disturbed–quiet–dst) exhibits variations of different time scales during the disturbed period (see Fig. 1(e)). It is also noticed from the figure that in the same time interval, SW density (Fig. 1(f)) also shows many enhancements and fluctuations. To the first speculation, we see some connection between the residual field and the SW parameters. The ground horizontal magnetic field variations although somewhat delayed, seem to follow the similar pattern as that of SW dynamic pressure/density. The SW density enhancements are shown by the upward arrows in the number density plot (Fig. 1(f)). Corresponding positive enhancements in the residual field at Alibag are shown by upward arrows, and negative perturbations are shown

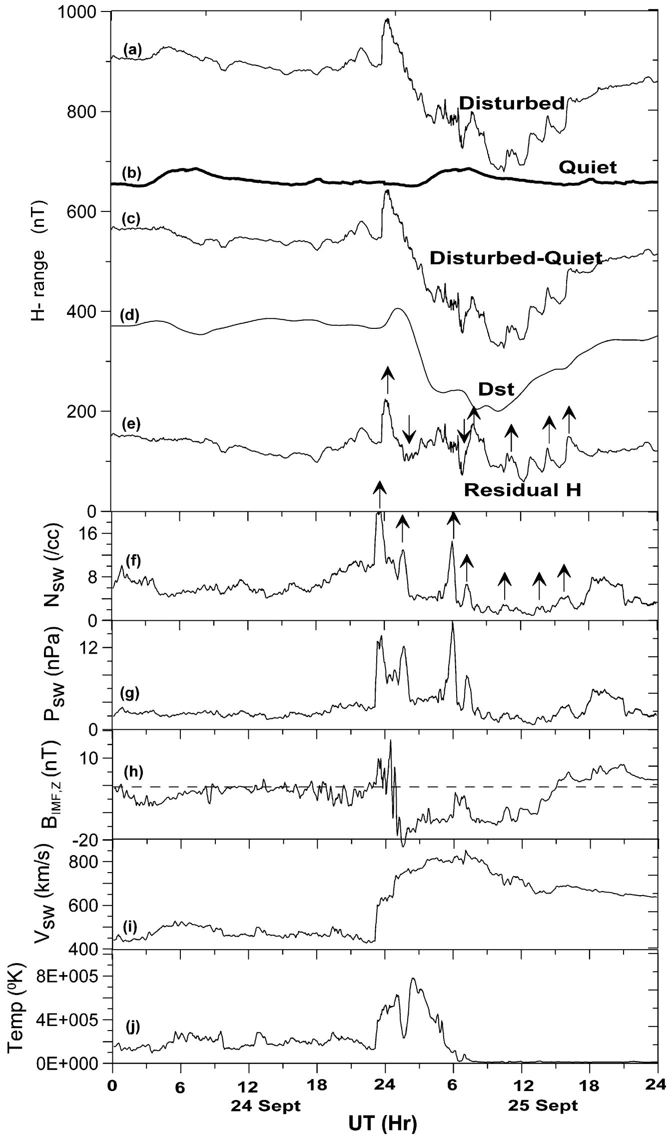

Fig. 1. The geomagnetic and SW parameters on 24–25 September 1998: (a) shows the horizontal magnetic field measurements at Alibag; quiet day (first quiet day of a month) variation is depicted in (b). Plot of Fig. (c) is obtained after removal of quiet day pattern from disturbed variation. Fig. (d) and (e) represent Dst-index and the residual field ((c)–(d)) respectively. Solar wind parameters are also shown (f): SW number density (N_{SW}), (g): dynamic pressure (P_{SW}), (h): Z-component of IMF ($B_{IMF,Z}$), (i): SW velocity (V_{SW}), and (j): Temperature are also shown at the bottom. Upward and downward arrows indicate the positive and negative enhancements respectively.

by downward arrows in Fig. 1(e). SW density enhancement at ~24 UT on September 24 (SSC), gives clear positive increase in the residual field; the IMF was northward during this time. The next positive pressure impulses at ~2 UT and 6 UT on 25 September with southward IMF result in negative variation (shown by downward arrows in Fig. 1(e)). Other SW density enhancements in the recovery phase of the storm have positive impact on the ground magnetic field. Thus, in general, it appears that out of all solar wind parameters, the SW dynamic pressure/density are better related to the ground geomagnetic field variations; nevertheless $B_{IMF,Z}$ also seems to play a role in controlling the type of impact, i.e., either positive or negative perturbation. Therefore, in this work, we intend to determine the most influential SW parameter for the ground magnetic field variations during entire storm time, by computing the correlation coefficient. Before employing the correlation technique, let us examine the power spectra, by subjecting the signals to a fast Fourier transform (FFT) analysis.

3. Spectral characteristics

In principle, one can use the fast Fourier transform (FFT) method for entire storm period (~48 h in the present investigation) to calculate spectra of the horizontal component of the magnetic field recorded on the ground and various SW parameters. But, power spectra for such a longer time interval could provide only the common frequencies during the entire storm period.

Figs. 2 and 3 show the power spectra for the variations on 24–25 September 1998 and 4–5 May 1998 respectively. Total 2048 data points with sampling rate of one minute are used in the present FFT analysis, which results in finer frequency resolution. Normalized power spectral density (PSD) of the H-component at Alibag station is shown at the bottom and, above that, PSD for various SW parameters are depicted. Above the power spectrum of each SW parameter, the relationship of it with that of the horizontal magnetic field at Alibag is shown by the coherence between the two (dotted curve). The coherence level of 0.9 is drawn by dotted horizontal line. In order to bring out the peaks with relatively smaller amplitude at higher frequency ranges, we have shown it separately on the right hand side (1.6–3.5 mHz in Fig. 2 and 1.2–3.5 mHz in Fig. 3) with enhanced scales (five times greater than that on the left hand side). Scales for the power spectrum are shown by an arrow, while that of the coherence coefficient are shown on the y-axis. Common frequency peaks between Alibag magnetic field and SW dynamic pressure are shown by vertical dashed lines.

On 24–25 September 1998, common spectral peaks between ground and SW pressure are observed at around 0.5, 0.65, 1.0, 1.2, 1.4, 1.8, 2.0, 2.4, 3.0, 3.2, 3.4 mHz. The common spectral peaks are also supported by the peaks in the coherence, most of the times attaining values above 0.9. Almost all these peaks are also evident in the SW density spectra. Though some of them are also present in other SW parameters such as peaks at around 1.0, 1.8 mHz seen in B_{IMF}, and peak at 2.4 mHz seen in $B_{IMF,Z}$; not all the frequency peaks are seen in other SW parameters. Nearly all the SW parameters show the spectral peak at around 0.5 mHz.

Similarly on 4–5 May 1998 (Fig. 3), common spectral peaks between H-Alibag and SW pressure are observed near 0.6, 0.8, 1.05, 1.3, 1.6, 2.0, 2.6, 2.8, 3.0 mHz. Analogous to the observations from previous figure, some of the spectral peaks are also evident in other SW parameters, e.g. peaks at 1.3, 2.0, 2.8 mHz are seen in $B_{IMF,Z}$; spectral peaks at 1.6, 2.0, 2.6 mHz are present in B_{IMF} and so on. Furthermore, it should be noted that small peak at 0.7 mHz in the ground data is not present in SW density/pressure but finds correspondence with $B_{IMF,Z}$ and $B_{IMF,Y}$; and also peak at 0.5 mHz in ground data is well connected with the SW temperature. Barring a few exceptions, the coherence is greater than 0.8 for all the peaks. That means, there are some frequency peaks seen at ground, which are associated with the SW parameters other than SW density/pressure. However, it is noted that most of the spectral peaks seen on the ground are associated with the SW density/pressure. To summarize, it is observed that in general, all the SW parameters show similar spectral structures during each individual event, but the similarity between the ground and SW density/pressure spectra appears to be the maximum.

It is evident from the study during all the six events that the power spectra of horizontal component of magnetic field at Alibag often shows the presence of discrete frequencies close to 1.3, 1.9, 2.6 and 3.4 mHz, which are also observed in SW dynamic

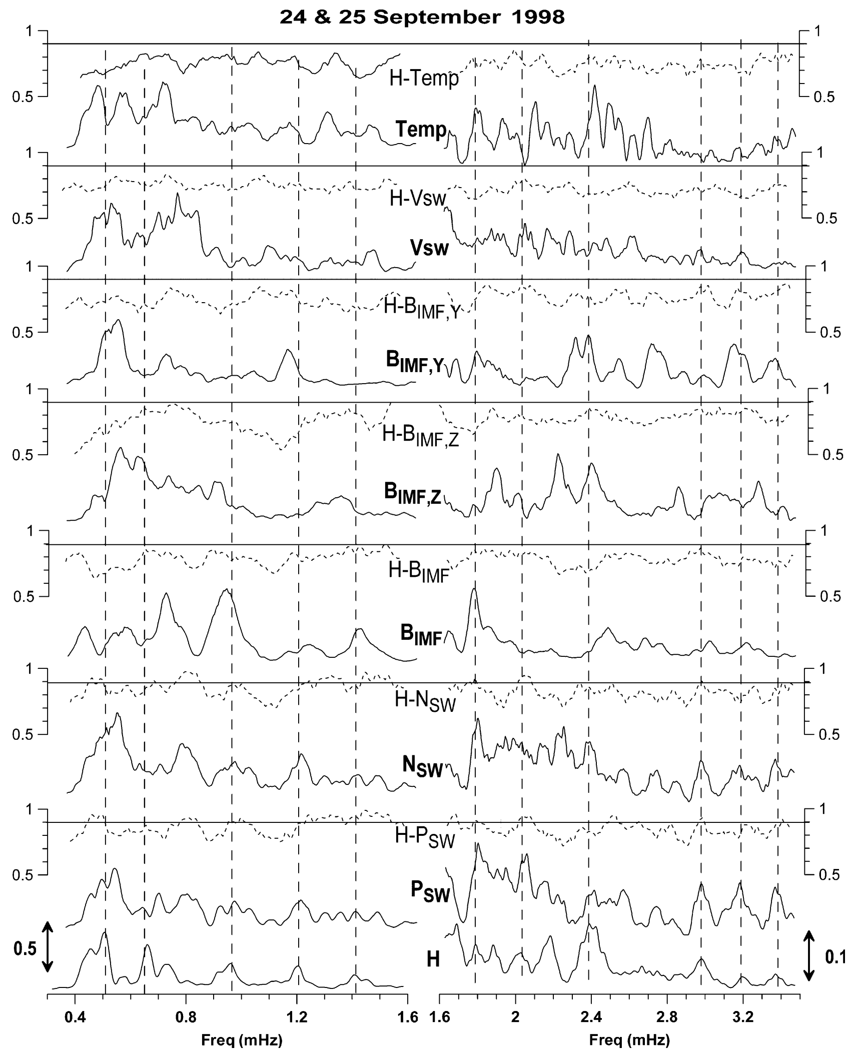

Fig. 2. (a) Bottom plot shows the power spectral density (PSD) of horizontal field at Alibag (H) on 24–25 September 1998, and above that PSD of various SW parameters are depicted. The coherence between each SW parameter and the horizontal field at Alibag is shown by the dotted curve on the top of each spectrum; the horizontal dotted lines represent coherence coefficient of 0.9. Frequency axis is divided into two panels; the right hand side panel (1.6–3.5 mHz) has enhanced scales (five times greater than that on the left hand side panel); the scales for each panel are shown by the arrows. *Y*-axes show the coefficient of coherence. Vertical dashed lines show the common frequency peaks between *H* and P_{SW}.

pressure/density. It should be noted that all these frequencies might not be present in each event. Independent study by Villante et al. (2007) also observed repeated occurrence of power enhancements in the low-latitude magnetic field variations in the same frequency bands, and found excellent correspondence of these frequencies with the SW variations. These discrete frequencies had been attributed to global magnetospheric MHD cavity and/or waveguide modes by earlier researchers (Kivelson and Southwood, 1986; Harrold and Samson, 1992). But later work showed that these frequencies could also be due to the directly driven response of SW variations (Kepko et al., 2002; Kepko and Spence, 2003). Present study confirms this driven response of the solar wind. We also observe other frequencies such as 0.5, 1.0, 1.4, 1.6, 2.0, 2.4, 3.0, 3.2 mHz present in the power spectrums of ground magnetic field and SW dynamic pressure/density. The coherence at the well-defined common peaks is better than 0.9. This may imply that the discrete frequencies observed in the ground measurements are due to the SW pressure variations.

In order to examine the temporal behavior of these frequencies, we perform time-frequency analysis to get dynamic spectrum. Though new time-frequency analysis technique using temporally confined base functions, called wavelet analysis is useful for detailed investigation, we employ here, a traditional short period Fourier transform using a sliding time window of 128 min and time step of 10 min. Fig. 4 shows dynamic spectra of various SW parameters and horizontal magnetic field at Alibag, for the storm during 24–25 September 1998. Spectrogram reveals burst-like character at ~24 UT. We observe that in general, the frequency enhancements in the interplanetary magnetic field (IMF) components and SW parameters are concurrent. In reality, it is quite common that the solar wind exhibits changes in its parameters and IMF often simultaneously. Passage of this solar wind disturbs the magnetic field variations on Earth and hence the enhanced activity is seen in the dynamic spectra of ground horizontal magnetic field. Broad range of frequencies is observed at ~24 UT. Then, all the SW parameters are nearly stable until about 30 UT (i.e., 06 UT on 25 September 1998). At ~06 UT, again high density SW plasma was observed. Dynamic spectra substantiate the effect of this second density/pressure burst in the ground magnetic field. Frequencies between 0.5 and 1 mHz are present through out the storm interval, in the horizontal component of ground magnetic field, which is also evident by the major spectral peaks in the power spectrum of Fig. 2.

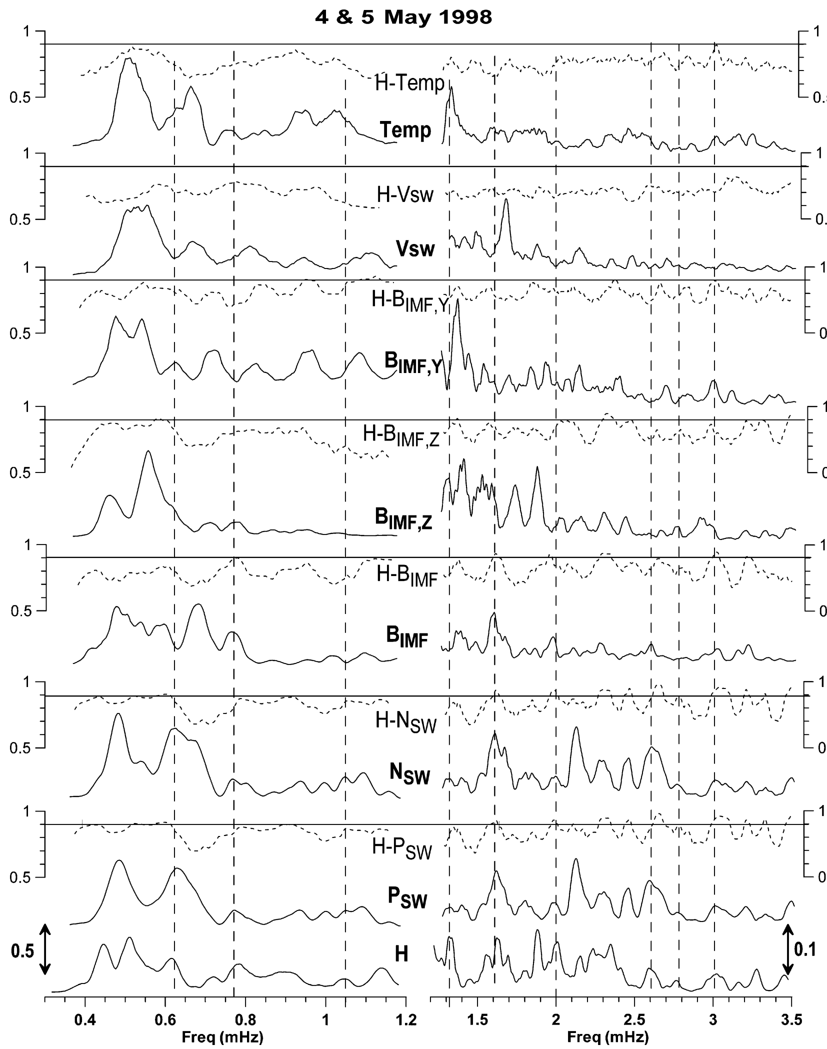

Fig. 3. Same as Fig. 2, but for 4–5 May 1998. In the left hand side panel, the frequency axis ranges from 0.3 to 1.2 mHz, while that in the right hand side panel varies from 1.2 to 3.5 mHz.

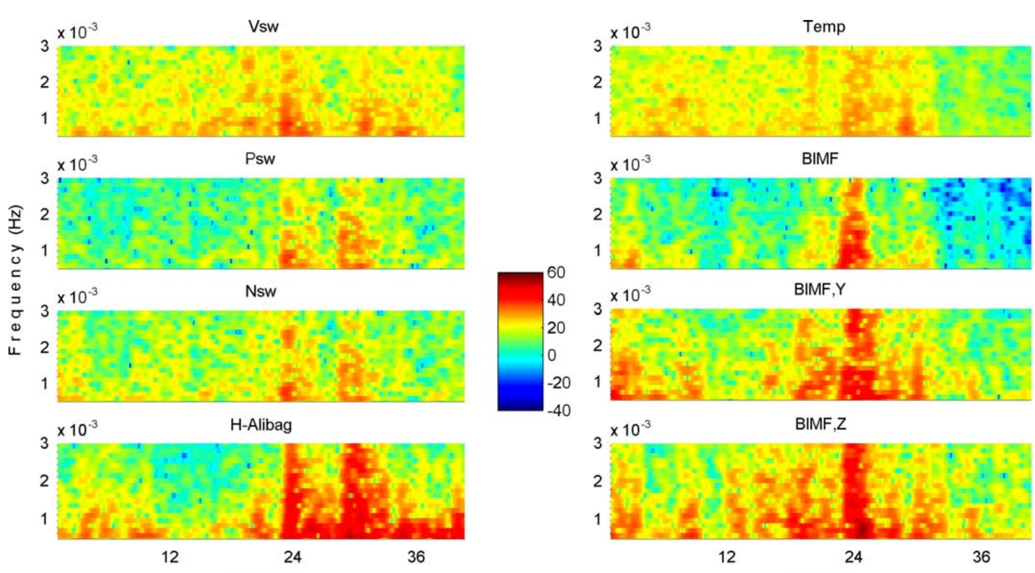

Fig. 4. Dynamic spectrum of various SW parameters and horizontal magnetic field at Alibag, during 24–25 September 1998.

4. Correlation analysis

Eventually, to confirm the visually identified result of previous sections quantitatively, we perform time-lagged correlation analysis on high-pass filtered time series. One-minute values of the geomagnetic horizontal components and SW parameters were high-pass filtered using a zero phase infinite-duration impulse response (IIR) filter. This digital filter reduces filter startup transients by carefully choosing initial conditions and uses the information in the signal at points before and after the current point, to eliminate phase distortion. The filter is stable with order of 172. The cut-off frequency of high-pass filter is selected at 0.4 mHz, allowing fluctuations smaller than 40 min. For performing the time-lagged correlation, we fix the time series of geomagnetic field at Alibag and move the time series of SW parameters forward.

Fig. 5 shows the correlation of Alibag magnetic field variations with various SW parameters as a function of time lag, for the event on 4–5 May 1998. Here we also use magnetic field measurements at Kakioka (Geomag. Latitude ~27.4°N, Geographic Longitude ~140°E) station to examine the correlation between two ground stations (shown by dotted curve with cross). It is found to be very high (0.8 for this event); and maximum correlation between these two is achieved at a time lag of 2 min. The maximum correlation coefficient (CC) between Alibag and Kakioka for other five events studied in this paper, not shown here, attains between 0 and 2 min, with excellent correlation (≥ 0.8) for all the cases. Also bear in mind that the latitudinal and longitudinal difference between Alibag and Kakioka is ~17° and ~67° respectively. Therefore the question is what does this imply—is this related to some globally driven phenomenon or does this suggest DP2 or substorm-type of current system responsible for this almost simultaneously observed signatures at such widely separated stations.

It is evident from the plots that out of all solar wind parameters, correlation is highest for SW dynamic pressure and density, shown by red curve with solid circles and black line with open squares respectively. The highest value of CC is around 0.45, at a time lag of 36 min. There are standard tests for testing the significance for the level of peak correlation obtained in each event. Since the time series considered in the present investigation for the correlation analysis comprise large data points covering two complete days, this is better than 99% in all the cases. It should also be noted that presence of wide range of frequencies could reduce the correlation coefficient. Fig. 6 shows the filtered time series using narrow band-passed filter for the frequency range of 0.5–1 mHz, which has been taken from Vichare and Alex (2006). It shows that each burst of SW density finds signature in the horizontal component of magnetic field at Alibag. It is evident from Fig. 6 that the signatures have one-to-one correspondence for each density pulse in the narrow band-passed filtered time series and hence have very high values of correlation coefficient (~0.8). Thus the correlation between narrow band-passed time series increases significantly.

Consequently, we observe that there is a high degree of resemblance between ground observations at low and mid latitude stations with wide longitudinal separation and SW dynamic pressure/density. This could suggest that the geomagnetic field variations are driven directly by the SW pressure/density changes. Similar conclusions have been drawn by Villante et al. (2007), who found one-to-one correspondence between ground, geostationary magnetospheric satellite and SW density variations. Since the ground magnetometers record the combined contribution from the current systems flowing above, such as magnetopause current, symmetric ring current (SRC), partial ring current (PRC), magnetotail current, and R1 and R2 region field-aligned currents, it is very difficult to decipher the most prevailing current system responsible for the observed geomagnetic field variation. Normally, the current system is deduced from the inspection of the type of geomagnetic response, viz., positive, negative or dipolarization type for each SW pressure impulses. In this scenario, the modeling efforts done by Shi et al. (2008a, b) are noteworthy. Assuming almost simultaneous response of the ground shorter time scale magnetic field variation is directly driven by the SW dynamic pressure enhancements, they modeled the response of different magnetospheric currents to the dynamic pressure enhancements during magnetic storms and compared with the ground magnetic field observations. They found that the

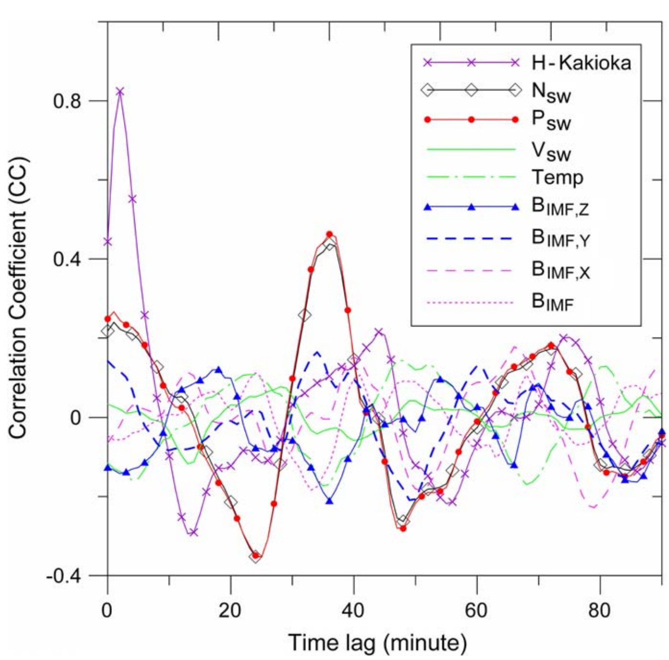

Fig. 5. Correlation coefficient of horizontal magnetic field at Alibag with various SW parameters and H-component at Kakioka as a function of time lag, during 4–5 May 1998. Very good correlation between two ground stations is evident. Out of all SW parameters, density and dynamic pressure (shown by black line with open squares and red curve with solid circles respectively) has highest correlation.

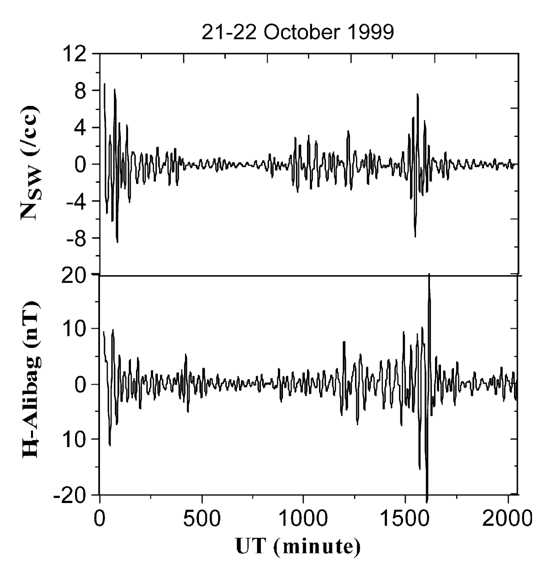

Fig. 6. Filtered time series for the frequency band between 0.5 and 1 mHz. (Vichare and Alex, 2006)

PRC and magnetopause currents are mainly responsible for the H-variations on the ground.

We have noted in the previous section that some of the spectral peaks present in the ground data are better associated with the SW parameters other than SW pressure/density. Therefore in the correlation analysis, we observe some correspondence of ground magnetic field variations with other SW parameters too, such as $B_{IMF,Z}$, $B_{IMF,Y}$, B_{IMF}, and SW temperature. However, the CC for SW pressure is significantly largest compared to other SW parameters during the entire storm interval.

Fig. 7 shows the time-lagged correlation between filtered series of Alibag magnetic field and SW dynamic pressure for all six intense storms studied in the present paper. It is observed that CC follows very systematic oscillatory pattern with respect to the time shift, which maximizes at ~30–45 min and decreases on both the sides; indicating that the signature observed by the ACE satellite gets recorded at the ground magnetometers after a time lag of ~30–45 min. Richardson et al. (1998) used the same method to estimate the propagation time of SW parameters between two different locations in space and they observed that the time lag depends on the radial and azimuthal separation; while Paularena et al. (1998) found corotation lags are not important. In the present scenario, this time difference can be explained as the sum of the radial propagation time from the satellite observation point, i.e., L1 point to the bow shock and the transmission time from the bow shock to the ground location. Since the SW velocity changes considerably over entire magnetic storm period, the time taken by each disturbance to reach bow shock and consequently to the Earth would vary, and hence for a longer data series as considered in the present study, it is not possible to get exact travel time. Just to get an averaged picture, we have plotted the time of maximum CC verses average SW velocity during each event, in Fig. 8. This shows that the time taken for the SW dynamic pressure variations to get recorded on Earth's surface at low latitude is inversely proportional to the solar wind velocity as one would intuitively guess. However it should be noted that the product of the delay time with the average SW velocity would not give the position of the ACE spacecraft, due to the rapidly varying nature of the SW velocity during storm interval. Similar correlation analysis was performed by Francia et al. (1999) between the square root of the SW pressure and low-latitude H-component during stable northward interplanetary magnetic field conditions. They compared the time lag of the highest correlation, which is the observed time delay, Δt, between Wind satellite and ground, with the radial propagation time τ, between Wind and the subsolar point of the bow shock and found difference of the order of a few minutes, which they interpreted as an additional transmission time from bow shock to the ground. For the present investigation, we cannot accurately evaluate τ, as SW velocity is highly variable during storm periods, unlike the steady conditions. However, we have repeated the same correlation analysis for the time interval with relatively stable SW velocity on 12 August 2000. The geocentric distance of ACE in Sun–Earth direction, X_{ACE} was 1.57×10^6 km. We found that the time lag for the highest correlation, Δt is equal to 43 min and the radial propagation time τ, between ACE and the subsolar point of the bow shock is around 41 min. Hence we obtain difference of about 2 min between observed time lag and the propagation time between ACE and subsolar point of bow shock, which is consistent with Francia et al. (1999). This additional time could be attributed to the transmission time from the bow shock to the ground.

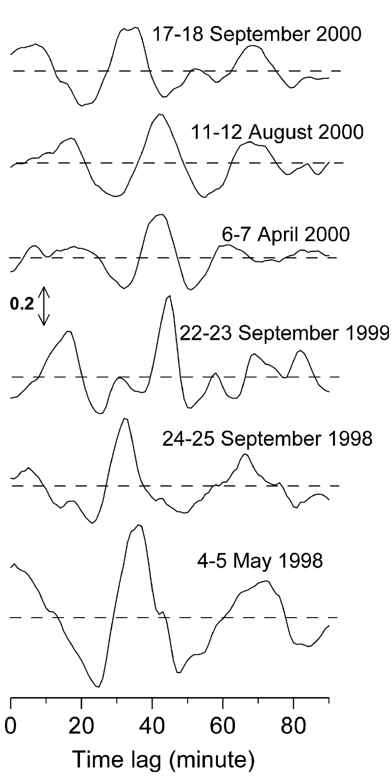

Fig. 7. Cross correlation between horizontal magnetic field at Alibag and SW dynamic pressure with respect to time lag, during all six geomagnetic storm events; scale is shown by an arrow. Dashed horizontal line represents zero line.

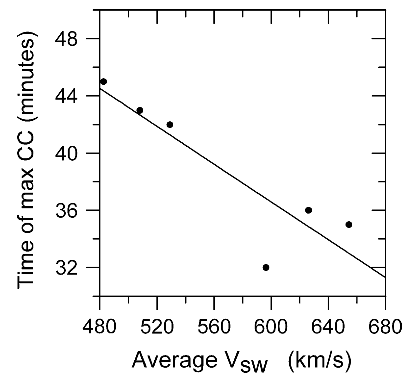

Fig. 8. Scatter plot of time of maximum coefficient of correlation against average solar wind velocity.

5. Day and night separation

In order to examine the local time dependence of the association of ground magnetic field variations with SW, we compute the correlation coefficient separately for day and night sectors. Fig. 9 shows the SW density for all six events considered in this paper. We have marked daytime and nighttime sectors as seen by Alibag. Thus, we have universal time range of 03–12 h as first day, and 27–36 h as second day, which makes LT range of 08–17 h at Alibag. Nighttime sector is represented by 13–25 UT (18–06 LT). Daytime sectors are highlighted between two adjacent vertical solid lines, whereas night sector lies between adjacent vertical dashed lines. The numbers shown in each sector represent the maximum correlation coefficient between SW density/pressure and the horizontal magnetic field at Alibag. It should be noted from the numbers that the correlations are not always good; it varies from poor association (CC = 0.1) to good one (CC = 0.5). It is found that on some occasions, nighttime correlations are higher than that during daytime; e.g. events on 17–18 September 2000, and 22–23 September 1999 indicate

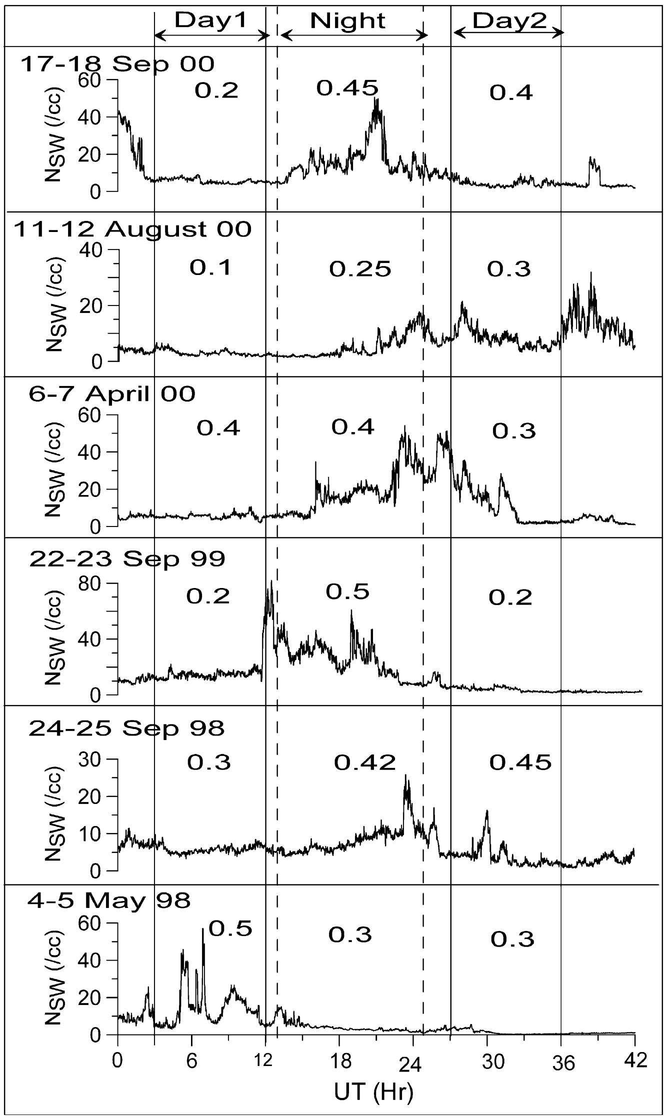

Fig. 9. Solar wind density plots for all six events, separated in day and night time sectors as seen at Alibag. Time intervals between two adjacent vertical solid lines indicate daytime, whereas that between dashed lines indicate night time interval. The numbers shown in each sector are the coefficient of peak correlation between SW pressure and horizontal magnetic field at Alibag.

better correlation during nighttime. However, there are other events, which show better correlation during daytime. Now let us examine the SW density variations during those times. It is clearly seen from the plots that correlation is more, during larger density variations. It has been reported by Richardson et al. (1998) that the degree of correlation between SW parameters seen at two different locations is determined by the standard deviation of the density. For the largest standard deviations of SW density, the correlation is highest. Our results seem to be consistent with these findings of Richardson et al. (1998). We report that the signatures of the stronger SW density enhancements are observed at low-latitude ground station, irrespective of day or nighttime.

6. Summary and discussion

Present paper examines the association of the geomagnetic field variations of shorter duration near equator with the SW changes, during six intense storm events, with the aid of ACE satellite measurements, which is located in the interplanetary medium and ground horizontal magnetic field data at Alibag observatory. The geomagnetic field response to the SW parameters could vary with the location. Most of the earlier studies have investigated the response at high to mid latitude stations, and none of the previous studies have utilized near equatorial station. Therefore, the magnetic field response at Alibag observatory is worth examining. During northward turning of the IMF, the geomagnetic response is merely of compression type, as a result of which a clean one-to-one association between SW pressure enhancements and the geomagnetic field variations is possible to obtain, which results in a very high value of correlation coefficient (Francia et al., 1999). On the contrary, the geomagnetic field response to the SW changes during southward turning of the IMF is complex due to the reconnection processes taking place at the dayside magnetopause and in the magnetotail region, and building up of the ring current (Shi et al., 2008a, b). Moreover, near the equator, the diurnal variations due to the ionospheric currents flowing overhead are very strong. Therefore, in order to study the Earth's magnetic field variations of the shorter time scale during entire storm interval, we systematically remove the longer period variations. The residual horizontal magnetic field obtained after removing the Dst and quiet time ionospheric variations from the ground magnetic data shows variations, which seem to follow almost similar pattern as that of SW pressure changes, although all the SW parameters exhibit variations during storm interval. Present study aims to identify out of all SW parameters, the parameter that correlates the best with the ground magnetic field variations of shorter time scales.

For this purpose, we employ the time-lagged correlation technique and compute the correlation coefficient between SW parameters observed at L1 point and horizontal magnetic field variations on the ground near equator. Thus, we deal with a correlation between two different quantities. Additionally, the properties of the SW parameters change considerably during its propagation from L1 point to the magnetosphere. Therefore, it is highly unfeasible to get CC close to one. Moreover, during storm period, IMF conditions are rapidly changing, and when IMF turns southward, additional currents such as magnetotail currents, field-aligned currents, and ring currents are set up in the Earth's environment; as a result of which the geomagnetic response does not remain simply of compression type. This reduces the value of CC between the ground magnetic field variations and SW density/pressure during storm time. The peak correlation between horizontal magnetic field at Alibag and SW pressure/density is found to be ~0.5 (Fig. 5), which is significant up to 99%, due to long time series (2 complete days) covering very large number of data points. Further, the value of peak CC increases considerably to 0.8 for narrow band-pass filtered data between 0.5 and 1 mHz and establishes one-to-one correspondence for each density pulse. Thus, we demonstrate that the dominant signatures observed in the horizontal component of the Earth's magnetic field near equator are well correlated with the SW dynamic pressure/density with an appropriate delay time between ACE and ground observations. The time lag required for the maximum cross correlation (~30–45 min for the present cases studied) indicates how much the time series of the SW parameters have to be shifted forward in time to get the best correlation with the time series of the ground magnetic field. This ultimately gives the good approximation of an averaged travel time between ACE and the ground magnetic station during entire storm interval, and is found to be proportional to the average SW velocity. Therefore, the driven global response of the magnetosphere can be monitored using low-latitude magnetic field observations. Furthermore, we note that other SW parameters, to some extent, also have influence on the low-latitude ground magnetic field variations. However, the value of CC between SW density/pressure and ground magnetic field (Fig. 5) is significantly larger than that of any other parameter of the solar wind. Thus, using the simple time-lagged correlation technique, the present study clearly demonstrates that out of all SW parameters, the SW density/pressure has most significant impact on the short time scale variations of the Earth's magnetic field, during entire storm interval.

It is known that the magnetic field variations recorded on the ground are manifestation of directly driven SW response as well as induced response. The power spectrums of ground H-magnetic field near the equator, for all storm events studied in the present paper, show the presence of discrete frequencies in a wide range from 0.5 to 4.0 mHz. Also recently, Viall et al. (2009) in their statistical study of over 10 years of SW number density and magnetospheric magnetic field data, have established the presence of discrete frequencies in the 0.5–5.0 mHz frequency range. According to the global magnetospheric cavity and waveguide models (Kivelson and Southwood, 1986; Harrold and Samson, 1992), the discrete frequencies of oscillations (1.3, 1.9, 2.6, 3.4 mHz) recorded near Earth are due to the properties of the magnetosphere. However, we observe that these frequencies (and also other frequencies such as 0.5, 1.0, 1.4, 1.6, 2.0, 2.4, 3.0, 3.2 mHz), are present in the solar wind data as well, which are far upstream from the Earth and hence cannot be considered as dependent on the magnetospheric features. The high coherence at common frequencies suggests that the discrete frequencies observed in the ground data are due to the SW variations. Viall et al. (2009) also found that many of the enhancements observed in the magnetospheric occurrence distribution of all statistically significant frequencies are similar to those seen in the SW number density, and further noted that certain discrete frequencies occur more frequently. Their results indicate the existence of inherent apparent frequencies in the SW number density. These findings thus illustrate the directly driven global response of the magnetosphere to the SW changes as reported by Kepko and Spence (2003), and Kepko et al. (2002), and present study confirms this using low-latitude ground magnetic field measurements. Although one cannot rule out the possibilities of other physical mechanisms through which the magnetosphere can oscillate.

From the separate investigation performed during day and night, though not always, we detect higher correlations between SW dynamic pressure/density enhancements and ground magnetic field even during nighttime. Further we notice that the correlation coefficients are higher during larger SW density variations (Richardson et al., 1998). This clearly indicates that the SW dynamic pressure enhancements of larger standard deviations recorded by the satellite located at L1 point have considerable impact on the magnetic field variations at the ground station near equator, irrespective of day or nighttime. This work can be further extended to compare the intensity of these ground signatures at daytime and nighttime stations simultaneously, for a given event. This could throw some light on the mechanism involved such as magnetopause, or superimposed ionospheric current systems responsible for the geomagnetic field response to the SW density enhancements. Shi et al. (2008a,b) used the modified modular Tsyganenko storm magnetic field model (TS04) as a tool to investigate the response of magnetospheric currents to the SW dynamic pressure enhancements during magnetic storms. They examined the contribution of each model current to the observed dawn–dusk asymmetric H-variations on the ground and found that the net field-aligned current system consisting of R1, R2 and the partial ring current closure, the equatorial portion of PRC and the magnetopause current are mainly responsible for the asymmetry.

Acknowledgments

We thank the Department of Science and Technology, India, under which the geomagnetic study is functioning. Authors would like to thank NSSDC at Goddard space flight center for making available the ACE satellite measurements. We thank the ACE SWEPAM instrument team, ACE magnetic field instrument team and the ACE science center for providing the data. We are also grateful to WDC-C2, Kyoto, for supplying ground magnetic field data, and Dst values. GSL thanks the Indian National Science Academy, New Delhi for the support under the Senior Scientist Scheme.

References

Chi, P.J., Russell, C.T., Musman, S., Peterson, W.K., Le, G., Angelopoulos, V., Reeves, G.D., Moldwin, M.B., Chun, F.K., 2000. Plasmaspheric depletion and refilling associated with the September 25, 1998 magnetic storm observed by ground magnetometers at $L = 2$. Geophys. Res. Lett. 27 (5), 633–636, doi:10.1029/1999GL010722.

Ebihara, Y., Ejiri, M., Nilsson, H., Sandahl, I., Milillo, A., Grande, M., Fennell, J.F., Roeder, J.L., 2002. Statistical distribution of the storm-time proton ring current: Polar measurements. Geophys. Res. Lett. 29 (20), 1969, doi:10.1029/2002GL015430.

Farrugia, C.J., et al., 2005. Interplanetary coronal mass ejection and ambient interplanetary magnetic field correlations during the Sun–Earth connection events of October–November 2003. J. Geophys. Res. 110, A09S13, doi:10.1029/2004JA010968.

Francia, P., Lepidi, S., Villante, U., Di Giuseppe, P., Lazarus, A.J., 1999. Geomagnetic response at low latitude to continuous solar wind pressure variations during northward interplanetary magnetic field. J. Geophys. Res. 104 (A9), 19923–19930, doi:10.1029/1999JA900229.

Fukushima, N., Kamide, Y., 1973. Partial ring current models for worldwide geomagnetic disturbances. Rev. Geophys. 11, 795–853.

Gonzalez, W.D., Tsurutani, B.T., Gonzalez, A.C., 1999. Interplanetary origin of geomagnetic storms. Space Sci. Rev. 88, 529–562.

Harrold, B.G., Samson, J.C., 1992. Standing ULF modes of the magnetosphere: a theory. Geophys. Res. Lett. 19, 1811.

Kivelson, M.G., Southwood, D.J., 1986. Coupling of global magnetospheric MHD eigen modes to field line resonances. J. Geophys. Res. 91, 4345–4351.

Kepko, L., Spence, H.E., Singer, H.J., 2002. ULF waves in the solar wind as direct drivers of magnetospheric pulsations. Geophys. Res. Lett. 29 (8)10.1029/2001GL014405.

Kepko, L., Spence, H.E., 2003. Observation of discrete, global magnetospheric oscillations directly driven by solar wind density variations. J. Geophys. Res. 108 (A6), 1257, doi:10.1029/2002JA009676.

Kleimenova, N.G., Kozyreva, O.V., Schott, J., Bitterly, M., Bitterly, J., 2002. Geomagnetic pulsations of the Pc5-6 range at equatorial and low attitudes. Geomagn. Aeron. 42 (4), 445–453.

Kokubun, S., 1993. Characteristics of storm sudden commencement at geosynchronous orbit. J. Geophys. Res. 88, 10,025.

Korotova, G.I., Sibeck, D.G., 1995. A case study of transient event motion in the magnetosphere and in the ionosphere. J. Geophys. Res. 100, 35.

Lee, D.-Y., Lyons, L.R., 2004. Geosynchronous magnetic field response to solar wind dynamic pressure pulse. J. Geophys. Res. 109, A04201, doi:10.1029/2003JA010076.

Liemohn, M.W., Kozyra, J.U., Thomsen, M.F., Roeder, J.L., Lu, G., Borovsky, J.E., Cayton, T.E., 2001. Dominant role of the asymmetric ring current in producing the storm time Dst*. J. Geophys. Res. 106, 10,883.

McPherron, R.L., O'Brien, T.P., 2001. Predicting geomagnetic activity: the Dst index. In: Song, P., Singer, H.J., Siscoe, G.L. (Eds.), Space Weather, Geophys. Monogr. Ser., vol. 125. AGU, Washington, D. C, pp. 339–345.

Moore, T.E., Peterson, W.K., Russell, C.T., Chandler, M.O., Collier, M.R., Collin, H.L., Craven, P.D., Fitzenreiter, R., Giles, B.L., Pollock, C.J., 1999. Ionospheric mass ejection in response to a CME. Geophys. Res. Lett. 26 (15), 2339–2342.

Nagano, H., Araki, T., 1986. Seasonal variation of amplitude of geomagnetic sudden commencements near midnight at geostationary orbit. Planet Space Sci. 34, 205.

Ogilvie, K.W., Burlaga, L.F., 1974. A discussion of interplanetary postshock flows with two examples. J. Geophys. Res. 79, 2324.

Paularena, K., Zastenker, G., Lazarus, A., Dalin, P., 1998. Solar wind plasma correlations between IMP 8, INTERBALL-1, and WIND. J. Geophys. Res. 103 (A7), 14601–14617.

Richardson, J., Dashevskiy, F., Paularena, K., 1998. Solar wind plasma correlations between L1 and Earth. J. Geophys. Res. 103 (A7), 14619–14629.

Rastogi, R.G., 1999. Signatures of storm sudden commencements in geomagnetic H, Y and Z fields at Indian observatories during 1958–1992. Ann. Geophys. 17, 1426–1438.

Russell, C.T., Ginskey, M., Petrinec, S., Le, G., 1992. The effect of solar wind dynamic pressure changes on low and mid-latitude magnetic records. Geophys. Res. Lett. 19 (12), 1227–1230, doi:10.1029/92GL01161.

Russell, C.T., Ginskey, M., Petrinec, S.M., 1994. Sudden impulses at low latitude stations: steady state response for southward interplanetary magnetic field. J. Geophys. Res. 99 (A7), 13403–13408, doi:10.1029/94JA00549.
Russell, C.T., Zhou, X.W., Chi, P.J., Kawano, H., Moore, T.E., Peterson, W.K., Cladis, J.B., Singer, H.J., 1999. Sudden compression of the outer magnetosphere associated with an ionospheric mass ejection. Geophys. Res. Lett. 26 (15), 2343–2346, doi:10.1029/1999GL900455.
Russell, C.T., Lu, G., Luhmann, J.G., 2000. Lessons from the ring current injection during the September 24, 25, 1998 storm. Geophys. Res. Lett. 27 (9), 1371–1374, doi:10.1029/1999GL003718.
Shi, Y., Zesta, E., Lyons, L.R., Boudouridis, A., Yumoto, K., Kitamura, K., 2005. Effect of solar wind pressure enhancements on the storm-time ring current asymmetry. J. Geophys. Res. 110, A10205, doi:10.1029/2005JA011019.
Shi, Y., Zesta, E., Lyons, L.R., Yumoto, K., Kitamura, K., 2006. Statistical study of effect of solar wind dynamic pressure enhancements on dawn-to-dusk ring current asymmetry. J. Geophys. Res. 111, A10216, doi:10.1029/2005JA011532.
Shi, Y., Zesta, E., Lyons, L.R., 2008a. Modeling magnetospheric current response to solar wind dynamic pressure enhancements during magnetic storms: 1. Methodology and results of the 25 September 1998 peak main phase case. J. Geophys. Res. 113, A10218, doi:10.1029/2008JA013111.
Shi, Y., Zesta, E., Lyons, L.R., 2008b. Modeling magnetospheric current response to solar wind dynamic pressure enhancements during magnetic storms: 2. Application to different storm phases. J. Geophys. Res. 113, A10219, doi:10.1029/2008JA013420.
Takahashi, K., Ukhorskiy, A.Y., 2007. Solar wind control of Pc5 pulsation power at geosynchronous orbit. J. Geophys. Res. 112, A11205, doi:10.1029/2007JA012483.
Tsurutani, B.T., Gonzalez, W.D., 1997. The interplanetary causes of magnetic storms: a review. In: Tsurutani, B.T. (Ed.), Magn. Storms, Geophys. Monogr. Ser., vol. 98. AGU, Washington, D. C, pp. 77–89.
Viall, N.M., Kepko, L., Spence, H.E., 2009. Relative occurrence rates and connection of discrete frequency oscillations in the solar wind density and dayside magnetosphere. J. Geophys. Res. 114, A01201, doi:10.1029/2008JA013334.
Vichare, G., Alex, S., Lakhina, G.S., 2005. Some characteristics of intense geomagnetic storms and their energy budget. J. Geophys. Res. 110, A03204, doi:10.1029/2004JA010418.
Vichare, G., Alex, S., 2006. Storm time magnetic field variations at low latitude and its association with solar wind parameters. In: Gopalswamy, N., Bhattacharyya, A., (Eds.), Proceedings of ILWS Workshop, ''Solar influence on the Heliosphere and Earth's environment: Recent progress and prospects. Goa, p. 245.
Villante, U., Francia, P., Lepidi, S., De Lauretis, M., Pietropaolo, E., Cafarella, L., Meloni, A., Lazarus, A., Lepping, R., Mariani, F., 1998. Geomagnetic field variations at low and high latitude during the January 10–11, 1997 magnetic cloud. Geophys. Res. Lett. 25 (14), 2593–2596.
Villante, U., Francia, P., Vellante, M., Di Giuseppe, P., Nubile, A., Piersanti, M., 2007. Long-period oscillations at discrete frequencies: a comparative analysis of ground, magnetospheric, and interplanetary observations. J. Geophys. Res. 112, A04210, doi:10.1029/2006JA011896.
Wang, C.B., Chao, J.K., Lin, C.-H., 2003. Influence of the solar wind dynamic pressure on the decay and injection of the ring current. J. Geophys. Res. 108 (A9), 1341, doi:10.1029/2003JA009851.
Zesta, E., Singer, H.J., Lummerzheim, D., Russell, C.T., Lyons, L.R., Brittnacher, M.J., 2000. The effect of the January 10, 1997, pressure pulse on the magnetosphere–ionosphere current system. In: Ohtani, S. (Ed.), Magnetospheric Curr. Syst., Geophys. Monogr. Ser., vol. 118. AGU, Washington, D. C, pp. 217.